Structural Engineering and Mechanics, *Vol. 59, No. 1 (2016) 15-36*
DOI: http://dx.doi.org/10.12989/sem.2016.59.1.015

Structural redundancy of 3D RC frames under seismic excitations

Ali Massumi[a] and Ramin Mohammadi[*]

Department of Civil Engineering, Faculty of Engineering, Kharazmi University, No. 43, Dr Moffateh Ave, Tehran 15719-14911, Iran

(Received November 15, 2015, Revised February 15, 2016, Accepted March 8, 2016)

Abstract. The components of the seismic behavior factor of RC frames are expected to change as structural redundancy increases. Most researches indicate that increasing redundancy is desirable in response to stochastic events such as earthquake loading. The present paper investigated the effect of redundancy on a fixed plan for seismic behavior factor components and the nonlinear behavior of RC frames. The 3D RC moment resistant frames with equal lateral resistance were designed to examine the role of redundancy in earthquake-resistant design and to distinguish it from total overstrength capacity. The seismic behavior factor and dynamic behavior of structures under natural strong ground motions were numerically evaluated as the judging criteria for structural seismic behavior. The results indicate that increasing redundancy alone in a fixed plan cannot be defined as a criterion for improving the structural seismic behavior.

Keywords: redundancy; overstrength capacity; ductility; seismic behavior factor; incremental dynamic analysis

1. Introduction

Redundancy has become a serious concern among engineers and researchers after the poor performance of structures, such as the collapse of a parking garage, during the 1994 Northridge earthquake. Since redundancy under seismic excitation is not thoroughly understood, the design recommendations for redundancy have been brought into question. The most commonly-accepted belief of redundancy is related to structural configuration. If the load is distributed among a large number of load bearing components, it is less likely for all components to fail at the same time. Other interpretations of redundancy have also been considered.

Redundancy can create alternative load paths to transfer the load from a damaged minor component to a major component of a structure to prevent its immediate collapse. The terms "redundancy" and "alternative load paths" are often regarded as synonymous (Marhadi and Venkataraman 2009). Redundancy is the ability of a structural system to redistribute a load which cannot be carried by the damaged members, on the other structural members (Biondini *et al.* 2008). Some researchers have defined an analytical parameter as redundancy according to the lines

∗Corresponding author, MSc, E-mail: ramin_mohammadi@live.com
[a]Associate Professor , E-mail: massumi@khu.ac.ir

http://www.techno-press.org/?journal=sem&subpage=8 ISSN: 1225-4568 (Print), 1598-6217 (Online)

of vertical seismic framing in any direction. ATC-19 and ATC-34 (1995) suggest that the reliability of the framing system against seismic loading depends on the number of lateral load-resistant components. It has been suggested that a response modification factor (R) can be divided into three parts: a strength factor (R_s), a ductility factor (R_μ), and a redundancy factor (R_R).

The factor ρ, known as the reliability/redundancy factor, was added to the NEHRP, UBC and IBC after 1997 and has been applied to the horizontal designs for earthquake loading since then. The mentioned factor is a function of the system configuration and the number of seismic components and does not depend on inherent structural parameters such as overstrength and ductility (Wen and Song 2003). Uncertainty in structural demand versus structural capacity is evident in most qualitative definitions of redundancy. Thus, most of these definitions have not been included in codes and seismic design of structures.

Bertero and Bertero (1999) studied structural redundancy and suggested that the degree of seismic redundancy for a structural system can be calculated as the number of plastic hinges occurred in a structural system which continues to yield until the structure exceeds the allowable limit, causing plastic displacement or complete collapse. They noted that redundancy produces several beneficial effects for the structural response to earthquake ground motion.

Wen and Song (2003) studied the reliability and redundancy of structural systems under SAC ground motion. They believed that when there are more elements involved in resisting lateral loading, the probability that all of the elements collapse at the same time is lower than when elements of equal resistance are involved. Husain and Tsopelas (2004) proposed the redundancy strength factor and the redundancy variation factor to measure structural redundancy of 2D RC frames.

Okasha and Frangopol (2010) investigated time variant redundancy of structural systems. They studied how structural reliability and redundancy were affected by the deterioration of structural resistance along with increasing in applied loading by using numerical examples. Kanno and Ben-Haim (2011) proposed a quantitative and widely-applicable concept of strong redundancy and showed its relation to the info-gap robustness of the structure.

Mohammadi *et al.* (2015) evaluated the probabilistic and deterministic effects of redundancy on both reliability and behavior factors of framed structures. They illustrated that the changes of two mentioned factors do not always follow the same manner due to the increasing of the structural redundancy.

In general, studies in the field of structural redundancy have been divided into probabilistic and deterministic approaches. Moreover, the effects of redundancy on the nonlinear behavior and seismic behavior factor (R) of previous investigations indicate that increasing the redundancy of framed structures is desirable for increasing R and improving seismic behavior, without considering its effects on ductility and overstrength capacity. The present study examined the effects of redundancy on R and structural seismic behavior in 3D RC frames with deterministic analysis. Case study frames with the same story area in their designs were chosen. To distinguish the roles of redundancy and total overstrength capacity, 3D frames were designed with equal ultimate lateral resistance and a base shear coefficient.

2. Sesmic behavior factor (R)

Although performance based design (PBD) is a more common method for designing and controlling structures, most of formal building design codes are based on force based design

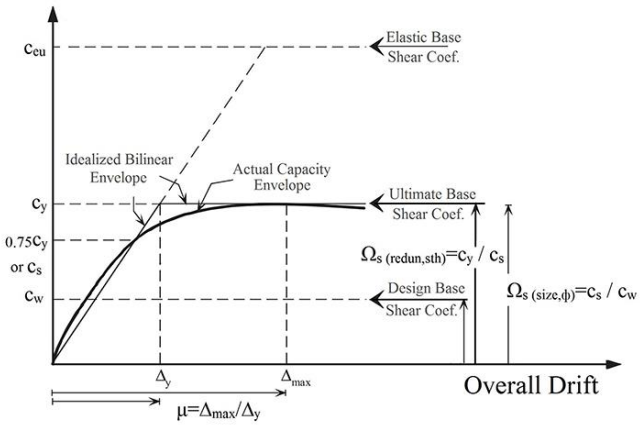

Fig. 1 Capacity curve and components of total overstrength factor

(FBD) methods in which seismic behavior factor is used. It should be noted that while designing a structure based on PBD, It is necessary to create a preliminary design of the structure, usually using FBD. Structural characteristics such as ductility, overstrength, and redundancy are measured to determine if structural systems with inelastic deformation and redistribution of forces can handle design earthquake input energy. These parameters are dependent on each other as well as the type of loading. In FBD in order to achieve the expected performance and dissipation of the earthquake energy with stable hysteretic behavior, structures having lateral force decreased by R should show specific values for redundancy, overstrength, and ductility. For achieving an accurate and adequate design using the seismic behavior factor, a structure should not encounter sudden and intense energy input in a short period of time which can disrupt the stable hysteretic plastic behavior of the structure (Kalkan and Kunnath 2007). Yang (1999) enhanced the accuracy and reliability of R by splitting it into separate factors. Most researchers and some seismic codes agree on factors such as ductility, overstrength capacity and redundancy (Massumi and Tasnimi 2006). The following conceptual formula has been proposed to calculate the seismic behavior factor

$$R_w = R_s R_\mu R_R = \left(\frac{c_y}{c_s} \times \frac{c_s}{c_w}\right) \times \frac{c_{eu}}{c_y} \times 1 \quad (1)$$

Where R_s is the total overstrength factor, R_μ is the ductility reduction factor, and R_R is the redundancy factor. R_R is also defined as the overstrength capacity from first significant yielding until total failure by some researchers (Husain and Tsoplas 2004, Fallah *et al*. 2009).

2.1 Total overstrength factor

Fig. 1 shows that the total overstrength capacity, which is created by a framed structural system, is composed of two parts. In the first part, the overstrength capacity forms from the design requirement for the base shear coefficient to the base shear coefficient for first local yielding. This component of total overstrength arises from the restricted choices for member sizes, rounding up of values for size and dimension, and differences between nominal and factored resistance. This is called the allowable stress factor and is calculated as (Yang 1991, Massumi *et al.* 2004)

$$\Omega_{s\,(size,\phi)} = \frac{c_s}{c_w} \quad (2)$$

In the second part, the overstrength capacity of the structure which is the result of structural redundancy and steel strain hardening, defined from first local yielding to total failure. When structural members begin to yield, the internal force is redistributed in response to structural redundancy and is affected by the failure mechanism. The overstrength capacity that forms after first local yielding until total failure is calculated as (Yang 1991, Massumi *et al.* 2004)

$$\Omega_{\mathrm{s\ (redu,sth)}} = \frac{c_y}{c_s} \tag{3}$$

The total overstrength factor is $R_s = \Omega_{\mathrm{s\ (size,\phi)}} \cdot \Omega_{\mathrm{s\ (redu,sth)}} = \frac{c_y}{c_w}$ using the allowable stress design approach and is $R_s = \Omega_{\mathrm{s\ (redu,sth)}} = \frac{c_y}{c_s}$ using the ultimate strength design approach (Yang 1991, Massumi *et al.* 2004).

2.2 Ductılıty reductıon factor

Fig. 1 shows the idealized capacity curve for an ideal elastic perfectly-plastic curve, the overall ductility capacity can be expressed as (Yang 1991, Massumi *et al.* 2004)

$$\mu = \frac{\Delta_{\max}}{\Delta_y} \tag{5}$$

Earthquake energy will depreciate in response to structural ductility. The energy dissipation capacity can decrease the elastic design forces to the level of total failure (yielding) as

$$R_\mu = \frac{c_{eu}}{c_y} \tag{6}$$

The present study used the results of research by Miranda, and Bertero (1994) for the analytical relation between μ and R_μ. The equation for the ductility reduction factor introduced by Miranda and Bertero was obtained from the study of 124 ground motions recorded on a wide range of soil conditions. The soil conditions were classified as rock, alluvium, and very soft sites which characterized by low shear wave velocity. A 5% of critical damping was assumed. The expressions for the period dependent ductility reduction factor $R_\mu$is calculated as

$$R_\mu\left(T,\mu\right) = \frac{\mu-1}{\phi} + 1 \tag{7}$$

Where ϕ is a function of the following three components: total ductility, the period of the system, and soil conditions. According to the method proposed by Miranda and Bertero, Φ is calculated as follow for the alluvium soil condition

$$\phi = 1 + \frac{1}{T(12-\mu)} - \frac{2}{5}\exp[-2(\ln T - 0.2)^2] \tag{8}$$

2.3 Redundancy factor

Different approaches exist to calculate the redundancy factor for R. Bertero *et al.* (1999) stated that the effects of redundancy and overstrength on R are not separable. They assumed that the redundancy factor is unity. Moreover, the combined effect of redundancy and overstrength expressed in terms of overstrength reduction factor. Structural redundancy is the primary component when calculating overstrength (Eq. (3)). So the secondary component of total

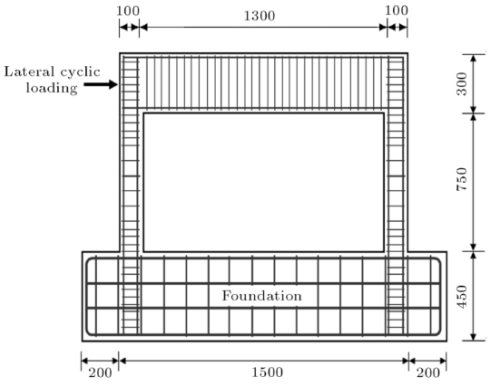

Fig. 2 Geometry of 2D RC frame

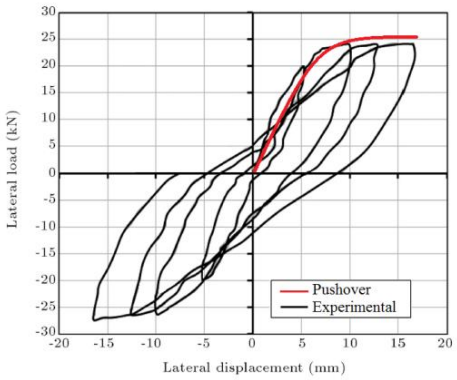

Fig. 3 Experimental and analytical response of 2D frame

overstrength introduced as redundancy factor by some researchers. Husain and Tsopelas (2004) and Fallah *et al.* (2009) introduced redundancy factor as additional strength from the formation of first local yielding until total failure using a simplified assumption. Although, the calculation of overstrength was not addresses in their study. Another parameter symbolized by ρ has been used in some codes as the redundancy factor which is based on the number of seismic resistant frames and the reliability of structures. In fact, ρ is the inverse ratio of R_R as calculated for the base shear coefficient of structural design. This coefficient is independent of total overstrength capacity (Liao and Wen 2004). The present study used both the allowable stress and ultimate strength methods to formulate the seismic behavior factor where the redundancy factor is considered to be unity. In this paper the number of lateral resisting elements in the building plan is used as the concept of redundancy.

3. Verification of analysis

In order to calibrate the analysis with experimental extracted date (Hashemi *et al.* 2009), a comparison between analytical and experimental data has been done. As shown in Fig. 2, the experiment was on a one story and one bay RC frame. Cyclic lateral load and constant gravity load are aplied. Fig. 3 indicates lateral load versus lateral displacement of roof. Adjustable parameters of the material are difiend so that the best calibration with the experimental data is acheived.

4. Models

Fig. 4 shows eight 3D RC special moment resisting frames with the same story areas and different numbers of floors and spans. Design base shear coefficient calculated based on the Iranian seismic design code (Standard 2800 2005) with the following assumption:

Level of seismicity is high. The importance factor of the structures is normal importance. (Residential buildings). Level of ductility is special. Soil profile is considered type II (Alluvium). Structures are regular in plan at all levels provided the seismic force-resisting systems consist of at least two bays of seismic force-resisting perimeter framing on each side of the structure in each

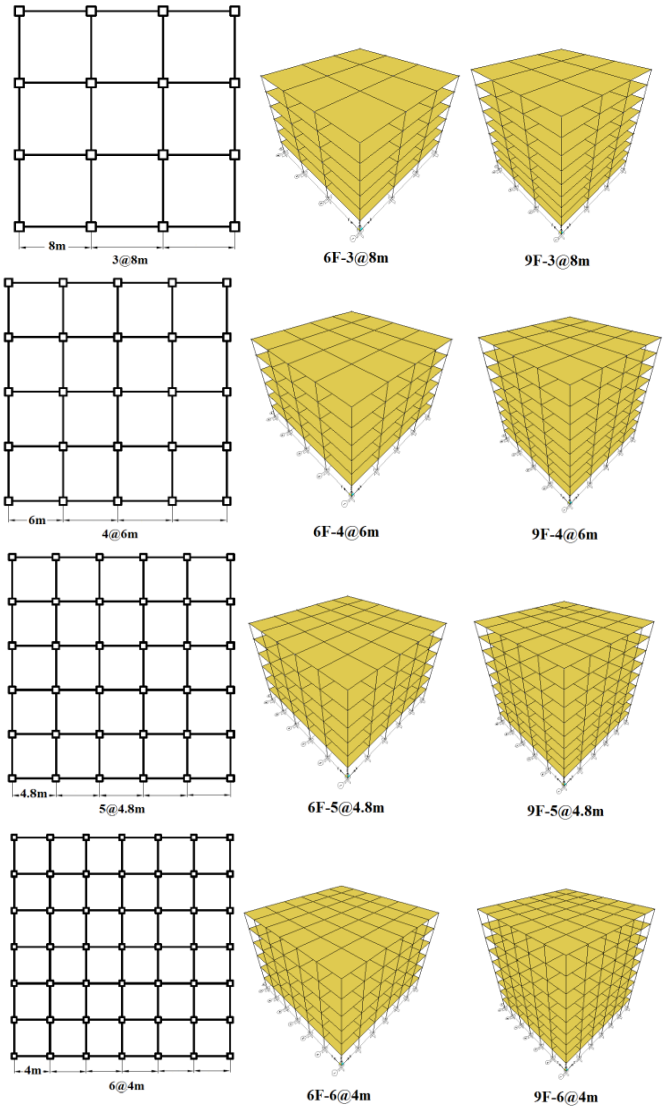

Fig. 4 3D reinforced concrete frames with different numbers of bays

orthogonal direction at each story resisting more than 35% of the base shear. So, the minimum number of element required for stability are provided are structures are redundant (ρ=1).

The floors area is 24 m×24 m for a range of spans with logical length of 4, 4.8, 6 and 8 m for different models. The numbers of floors are six and nine. The story height is 3 meter. A two-way concrete slab system, commonly used for floors of conventional buildings, is used here. The loads are applied according to Iranian National Building Code Part 6 and code 2800. SAP2000 software, which is a structural analysis and design tool, is used for the design and nonlinear incremental static and dynamic analysis. From hystertics models of FEMA356, interacting P-M_2-M_3 is used for the nonlinear behavior of columns and moment M_3 shear V_2 is used for the nonlinear behavior of beams.

The models were designed for incremental increases in lateral loading with an inverted triangular distribution and the constant gravity loads. The ultimate base shear coefficient and ultimate lateral resistance of the models were equal when the level of overall drift reached 2.5%.

An iterative process of trial and error was used for selecting the sections and analyzing, designing, and determining the section reinforcement in order to produce identical values for the ultimate base shear coefficient and ultimate lateral resistance of the models. The total overstrength factor $R_s = \Omega_{s\,(\text{size},\phi)} . \Omega_{s\,(\text{redu,sth})}$, is the same for the six- and nine story models by using the aforementioned design procedure. It was concluded that any changes in the amount of the calculated R does not depend on R_s. However, it depends on the ductility reduction factor for the specific number of bays (redundancy). The equivalent lateral resistance and equal base shear coefficient in the models distinguish the role of redundancy and total overstrength reduction factors.

5. Performance criteria

Performance criteria should be defined for structures or structural components to monitor responses during the procedure of analyzing and estimating *R* for the structures. Limitations imposed to stop nonlinear static pushover analysis.

5.1 Interstory drift

The interstory drift ratio was limited to 2.5% for nonlinear static analysis. The allowable value for this criterion is between 2% to 3%, as it is mentioned in most seismic building codes. Previous researches have shown that RC resisting moment frames have the capacity to increase overstrength after attaining an interstory drift of 2%. However, it cannot increase overstrength when interstory drift exceeds 2.5% (Massumi *et al.* 2005). Although designs based on standard 2800 are force based designs, the design methodology complies with the life safety performance level for residential buildings. Some codes, such as IBC, reach an interstory drift of ~2.5% to comply with collapse prevention performance levels. In this study, the calculated *R* and its components are based on an interstory drift of 2.5%.

5.2 Structural instability caused by hinge formation

This criterion is used when instability occurs in all or part of a structure in response to the hinge formation mechanism and when the stability index exceeds $\theta_{\max}$. The Iranian seismic code defines the stability index as follow

$$\theta_{\mathrm{i}} = \frac{\Delta \mathrm{Vi}}{\mathrm{Vi}} = \left(\frac{\mathrm{P}\Delta}{\mathrm{Vh}}\right)_{\mathrm{i}} \tag{9}$$

where ΔV_i is the shear added in the i^{th} floor created by *P*-Δ effects, P_i is the total dead and live loads for the i^{th} floor and higher floors, Δ_i is interstory drift for the i^{th} floor, $\mathrm{H_i}$ is the height of the i^{th} floor and

$$\theta_{\max} = \frac{1.25}{\mathrm{R}} \leq 1.25 \tag{10}$$

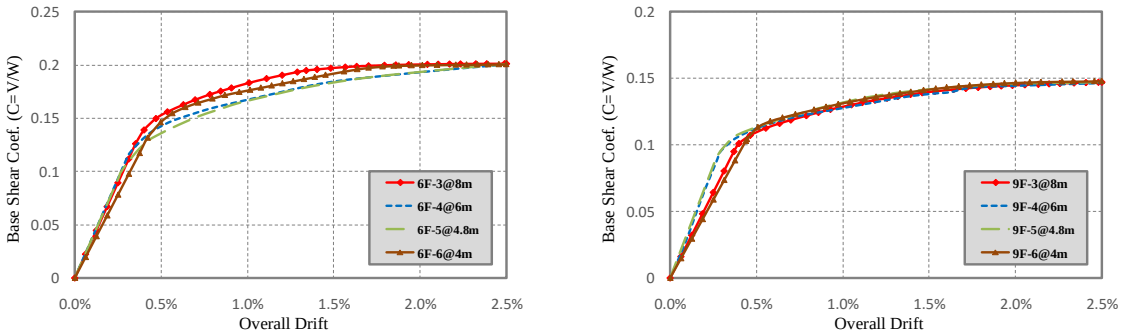

(a) 6-floor (b) 9-floor

Fig. 5 Capacity curves of: (a) 6-floor; and (b) 9-floor structures

Table 1 R for the allowable stress and ultimate strength approaches

Ref. Code	T	C_w	C_s	C_y	Δ_s	Δ_y	$\Omega_{s\,(redu,sth)}$	$\Omega_{s\,(size,\phi)}$	R_s	μ	R_μ	R_w	R
6F-3@8m	1.13	0.0756	0.1261	0.2013	0.0035	0.0057	1.597	1.648	2.632	4.4	5.42	14.27	8.67
6F-4@6m	1.09	0.0756	0.1111	0.2003	0.003	0.0054	1.803	1.456	2.625	4.6	5.73	15.04	10.33
6F-5@4.8m	1.07	0.0756	0.1006	0.2004	0.0027	0.0054	1.992	1.315	2.620	4.6	5.73	15.01	11.41
6F-6@4m	1.2	0.0756	0.1317	0.2008	0.0042	0.0065	1.525	1.722	2.625	3.8	4.7	12.34	7.17
9F-3@8m	1.61	0.0624	0.0951	0.1472	0.0037	0.0058	1.548	1.524	2.358	4.3	4.82	11.37	7.46
9F-4@6m	1.38	0.0624	0.0906	0.1468	0.0028	0.0044	1.587	1.486	2.358	5.7	6.62	15.61	10.50
9F-5@4.8m	1.39	0.0624	0.0864	0.1470	0.0026	0.0044	1.701	1.385	2.356	5.7	6.6	15.55	11.23
9F-6@4m	1.68	0.0624	0.1030	0.1479	0.0044	0.0063	1.437	1.641	2.359	4.0	4.39	10.36	6.31

6. Nonlinear static analysis

The structures were analyzed under incrementally increasing lateral loads with inverted triangular distributions and constant gravity loads in order to estimate the ductility ratio, overstrength factor, allowable stress factor, and seismic behavior factor under static inelastic loading. Lateral loading was applied so that 100% of the forces and displacement in one direction and 30% of the forces in the vertical direction contribute to the third dimension of the structural system when computing the ductility ratio and overstrength factor. To design the members' size and the amount of reinforcement, a trial and error approach was used. The ultimate strength of structures under these loading conditions is equal when the overall drift reaches 2.5%.

Fig. 5 shows the capacity curves for the 6- and 9-floor structures. The bilinear idealization of the capacity curve was obtained using the recommendations given by Park (1989) for RC members. The effective elastic stiffness was obtained as the slope value of the line connecting the origin to either the point of first yielding or 75% of the ultimate load, whichever is less.

6.1 Results of nonlinear static analysis

The results of static pushover analysis were evaluated to establish the components of R. Table 1 shows the values and components for R using the allowable stress and ultimate strength approaches. As seen, the values of the ultimate base shear coefficient (c_y) and the total overstrength

factor (R_s) are approximately equal.

Fig. 6 demonstrates the variation in the overstrength factor versus the number of bays in the 6- and 9-floor models. The overstrength factor first increased as the number of spans increased and eventually it decreased. The overstrength factor should not be expected to increase as the redundancy increases in a fixed plan because of the decline in local ductility of the members and the effects of the third dimension when computing it. Fig. 7 shows that the variation in allowable stress is inversely related to the variation in overstrength.

Fig. 8 indicates that the total overstrength is equal for the bays of both the 6- and 9-floor models. Fig. 9 shows that increasing in the number of spans from 3 to 4 in each direction would lead to a rise in the ductility reduction factor. It remains relatively constant as the number of spans increased from 4 to 5. However, increasing the number of spans from 5 to 6 in each direction

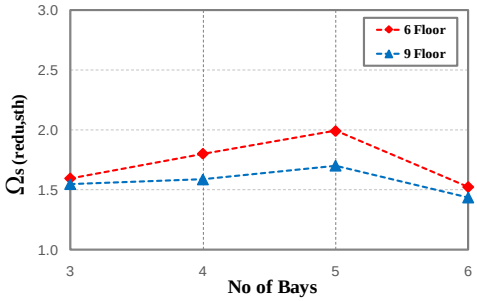

Fig. 6 $\Omega_{s\ (redu,sth)}$ vs. number of bays in each direction

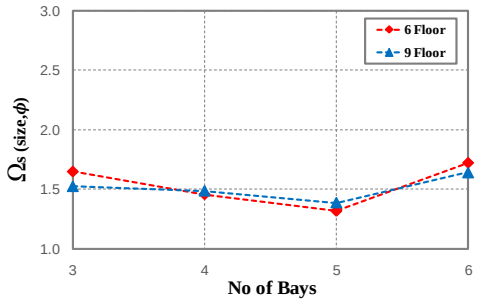

Fig. 7 $\Omega_{s\ (size,\phi)}$ vs. number of bays in each direction

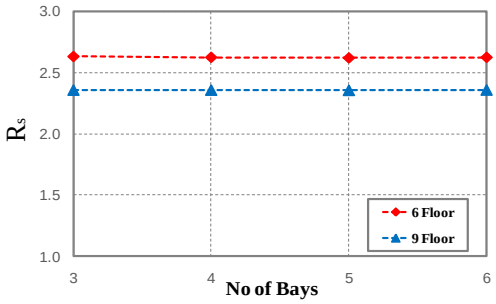

Fig. 8 R_s vs. number of bays at each direction

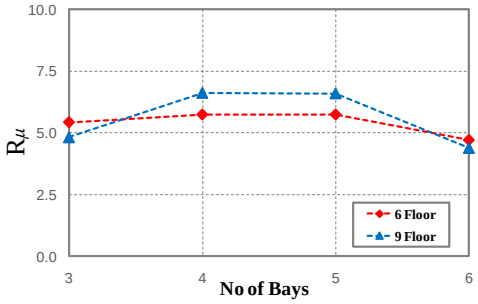

Fig. 9 R_μ vs. number of bays in each direction

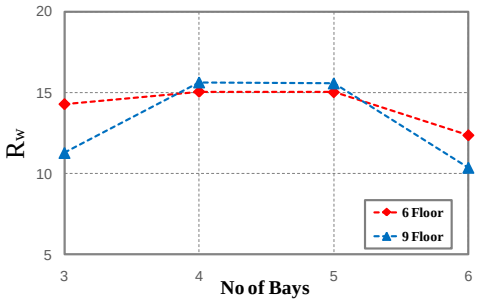

Fig. 10 R_w vs. number of bays in each direction

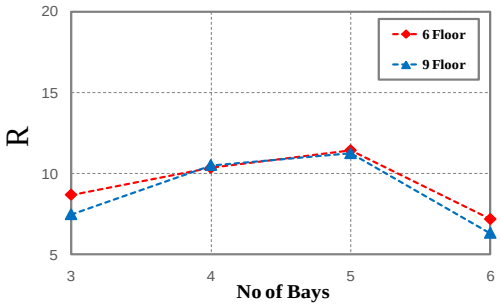

Fig. 11 R vs. number of bays in each direction

decreases the ductility reduction factor.

Figs. 10 and 11 indicate the variation in seismic behavior factor with allowable stress design and ultimate stress design, respectively, versus the number of bays. These graphs represent that increasing the redundancy in the structures cannot always contribute to the increase in R.

Figs. 6 to 11 show that for designing structures with same ultimate lateral strength, the smaller the force at the formation of the first plastic hinge is, the greater the value of ductility (μ) and overstrength factor ($\Omega_{s\,(\mathrm{redu,sth})}$) would be. If increasing in redundancy of a fixed plan leads the structural system to form the first plastic hinge at lower force levels, it can be concluded that an increase in redundancy will result in an increase in R. However, any increases in redundancy cannot be considered as a positive effect on increasing R. Therefore, it is necessary to study how other components of R, especially ductility, are affected by increase in redundancy. Excessive redundancy in a fixed plan can decrease the local ductility of members and cause components to behave in force control manner. It can also decrease the overall ductility ratio.

7. Nonlinear dynamic analysis and seismic behavior

The computed R is based on monotonic loading in static nonlinear analysis and may not reflect realistic structural seismic behavior. It must be determined that under which circumstances the seismic input energy of structures dissipates due to the stable hysteretic behavior and how this relates to redundancy. Herein the accuracy of the computed R was verified by incremental nonlinear dynamic analysis of structures as the criterion for structural seismic behavior.

The accelerograms consisted of near field and far field earthquakes records. The presence or absence of high amplitude and long period pulses in the velocity time history of an earthquake record, which contains very high kinetic energy, was a criterion for selecting that type of strong ground motion. High amplitude and long period pulses in the velocity time history are important

Table 2 Selected earthquake records

Earthquake Names/Station	Duration (s)	Distance (km)	PGV (cm/s)		PGA (g)	
			LN*	TR**	LN	TR
Tabas 1978, Tabas	22	3	97.8	121.2	0.836	0.852
Bam 2003, Bam	12	1	59.2	121.5	0.623	0.778
Kocaeli 1999, Yarimca	13	2.6	66.1	62.44	0.268	0.349
North Palm Springs 1986, NPS Station	10	2.8	33.8	73.24	0.694	0.594
Superstition Hills 1987, Parachute Test Site	18	0.7	43.9	112	0.377	0.455
Whittier Narrows 1987, Santa Fe Springs	20	10.8	21.3	37.7	0.443	0.426
Loma Prieta 1989,Saratoga Valley	12	13.7	42.5	61.54	0.255	0.332
Northridge 1994, Saticoy St.	14	13.3	28.9	61.47	0.368	0.477
Northridge 1994, Sun Valley (Roscoe Blvd)	12	12.3	22.1	38.21	0.303	0.444
El Centro 1940	30	12.99	11.67	29.69	0.215	0.313
Big Bear 1992, Big Bear Lake	20	10.15	27.97	33.50	0.472	0.534

* LN: Fault Parallel component

** TR: Fault Normal component

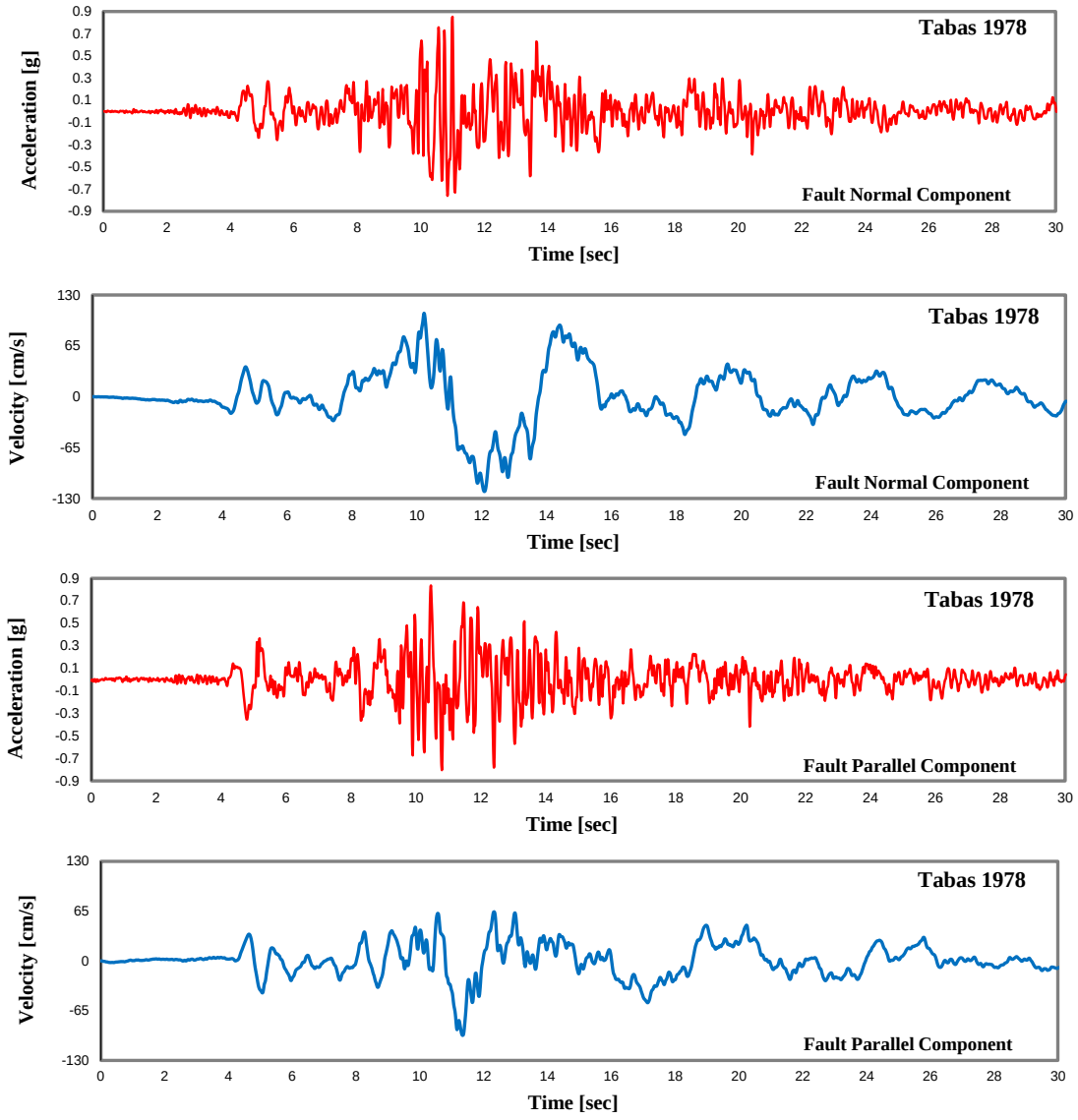

Fig. 12 Acceleration and velocity time history of Tabas earthquake

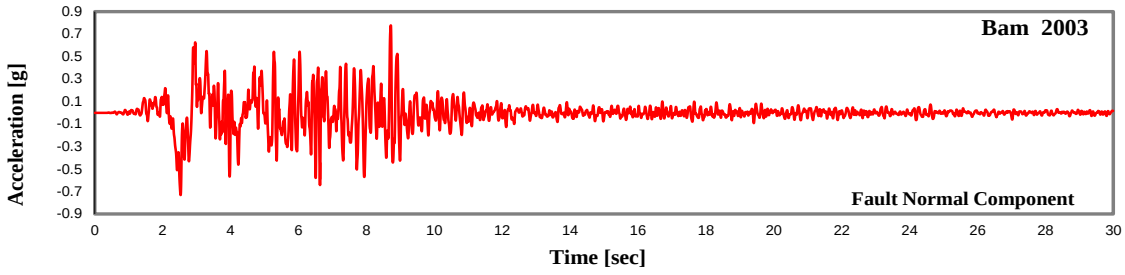

Fig. 13 Acceleration and velocity time history of Bam earthquake

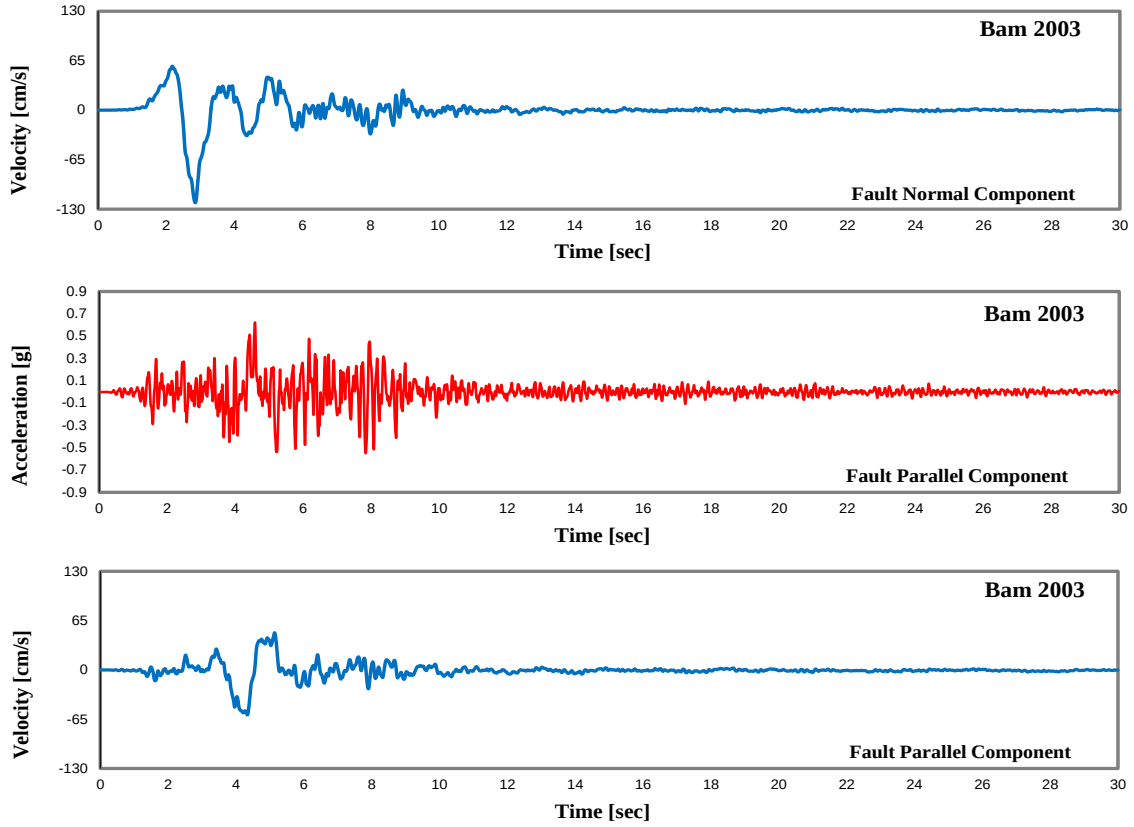

Fig. 13 Acceleration and velocity time history of Bam earthquake

disruptive factors affecting plastic stable hysteretic behavior.

Most seismic design codes do not consider the peak ground velocity (PGV) and the effects of field on the earthquake wave record. Researches show that PGV and kinetic energy input are significant parameters required for the seismic design of structures (Kalkan and Kunnath 2007).

Table 2 shows the selected earthquakes and their peak ground acceleration (PGA) and PGV.

Figs. 12 to 14 show the acceleration and velocity time histories of three records with high amplitudes and long period velocity pulses.

Fig. 15 shows the velocity response spectra of the records. Incremental nonlinear dynamic analysis with a bi-directional strong ground motion component for the earthquakes listed in Table 2 was used to study the compatibility of structural nonlinear behavior with R. The components of earthquake records with larger PGAs were applied to the X direction of the plan and those with smaller PGAs were applied to the Y direction. Structural response parameters for nonlinear deformation such as story drift, velocity, and story acceleration are presented for the three different scales of acceleration records. The scale factors were chosen in a way that structures under the applied accelerograms reached the three performance levels (B-IO, IO-LS, LS-CP) based on FEMA356. The response parameters indicate that structures with larger R showed relatively better performance under seismic excitation. However, there is no criterion for the relation between R and the seismic performance of the structures after achieving a certain level of performance. The

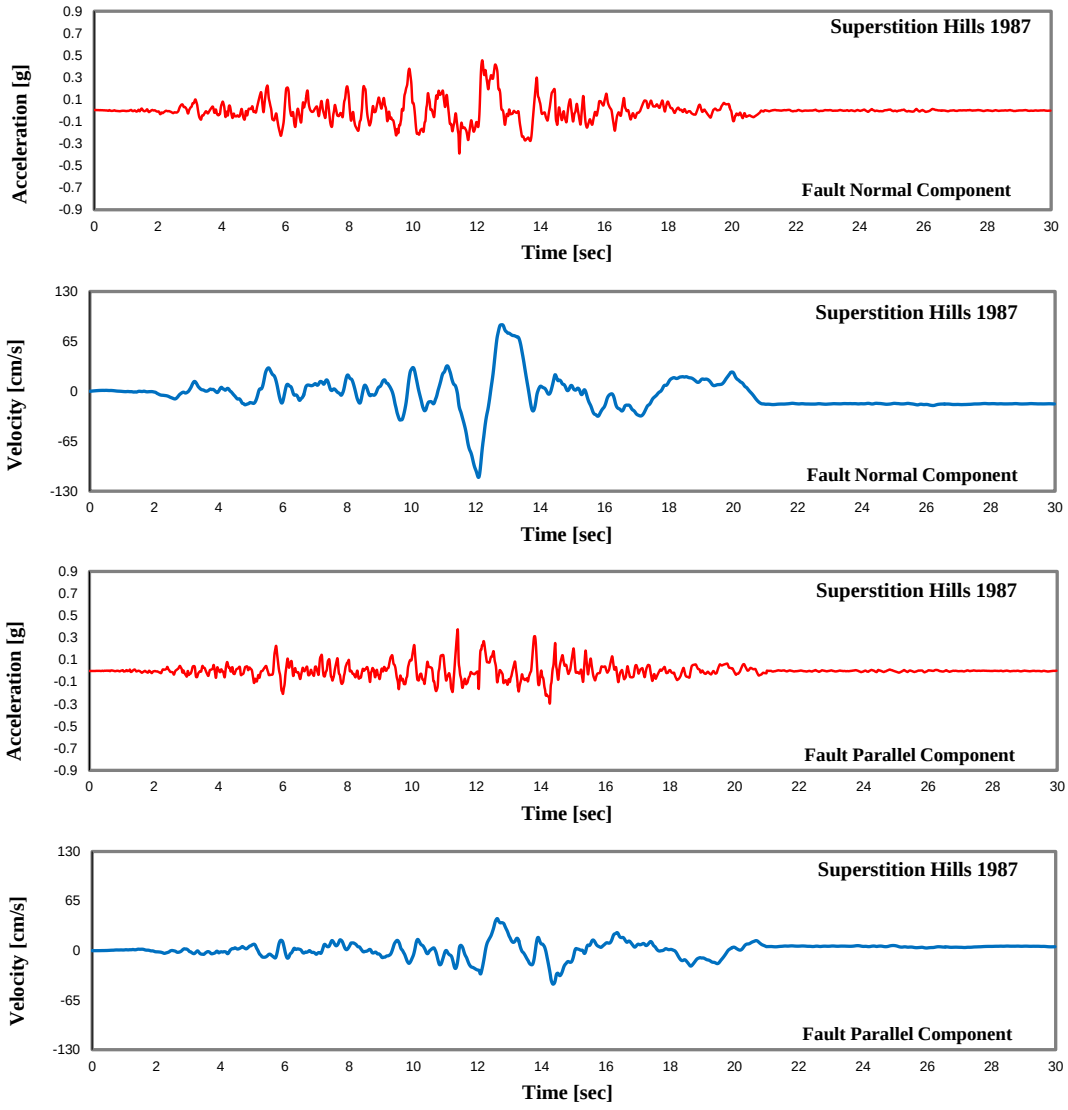

Fig. 14 Acceleration and velocity time history of SuperstitionHills earthquake

results of dynamic analysis reveal a limitation in the seismic behavior factor for reflecting the seismic behavior of the structures.

7.1 Nonlinear dynamic response of structures

Output from the dynamic response of structures in X and Y directions of each structure were studied. Figs. 16 to 26 illustrate the interaction of maximum acceleration, maximum velocity, and maximum drift of each story on a three-factor scale. Figures related to the directions of the structure in which the structural response is critical, are presented.

The structural response parameters represent the limitations of R as criteria for structural

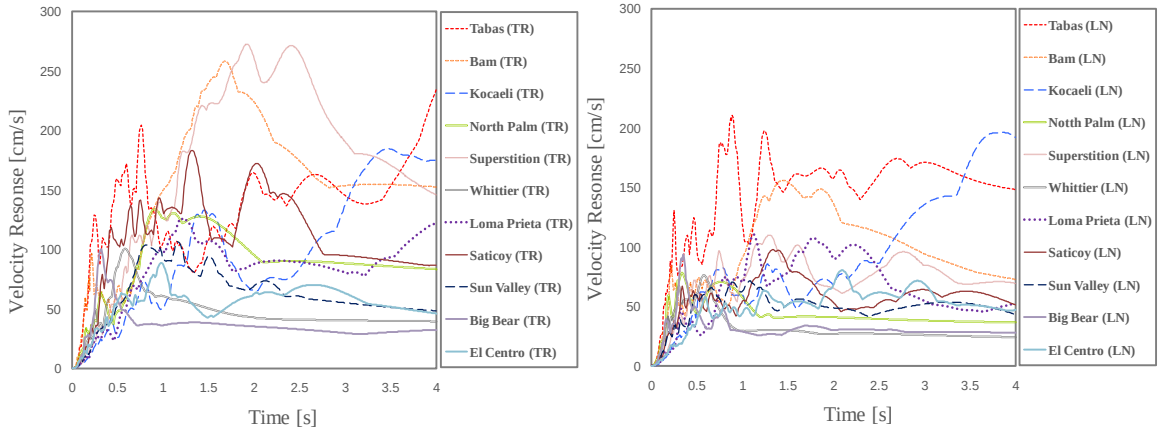

Fig. 15 Velocity response spectra of earthquake records from Table 2

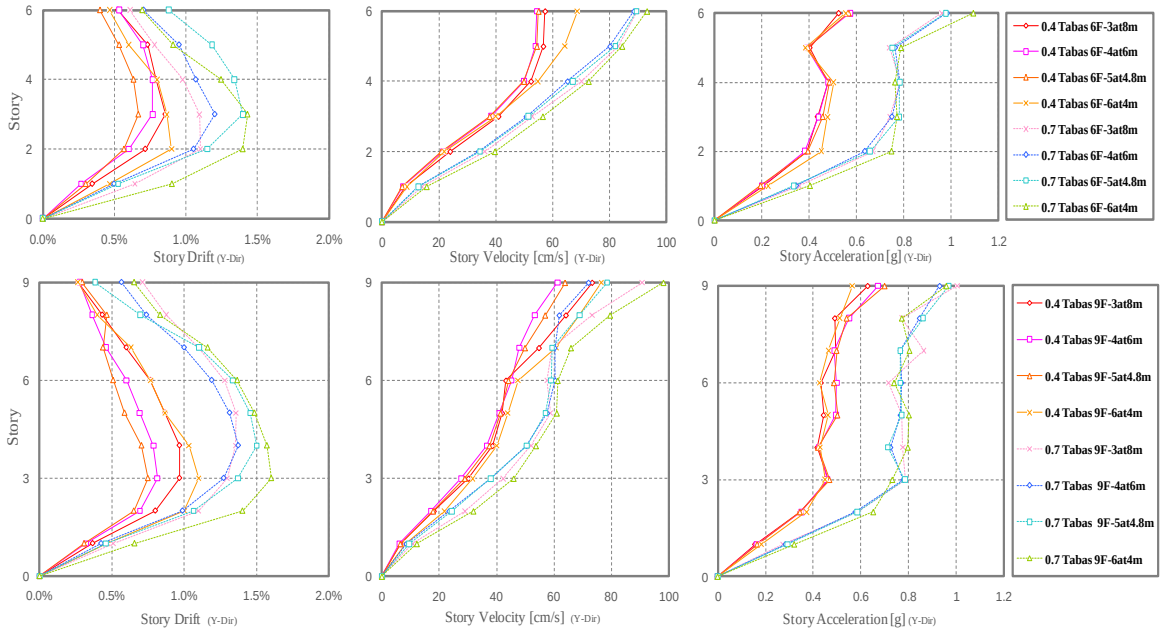

Fig. 16 Maximum story drift, velocity, and acceleration from Tabas earthquake

seismic behavior. It is reasonable to expect that structures with larger R values perform more favorably under earthquake loading. However, the results indicated that structural behavior does not always correspond to R. It has been shown in the results that when the structural demand decreases in comparison to the structural capacity, the seismic behavior typically follows R. Moreover, when structural demand increases in comparison to the structural capacity, the seismic behavior of the structure does not follow R.

Structural seismic behavior generally follows the calculated R under excitation for the records that provide story drift of ~1.5%. Although, the response parameters of structures do not follow the calculated R for powerful earthquake records that create story drift of 1.5% to 2%. It was noted

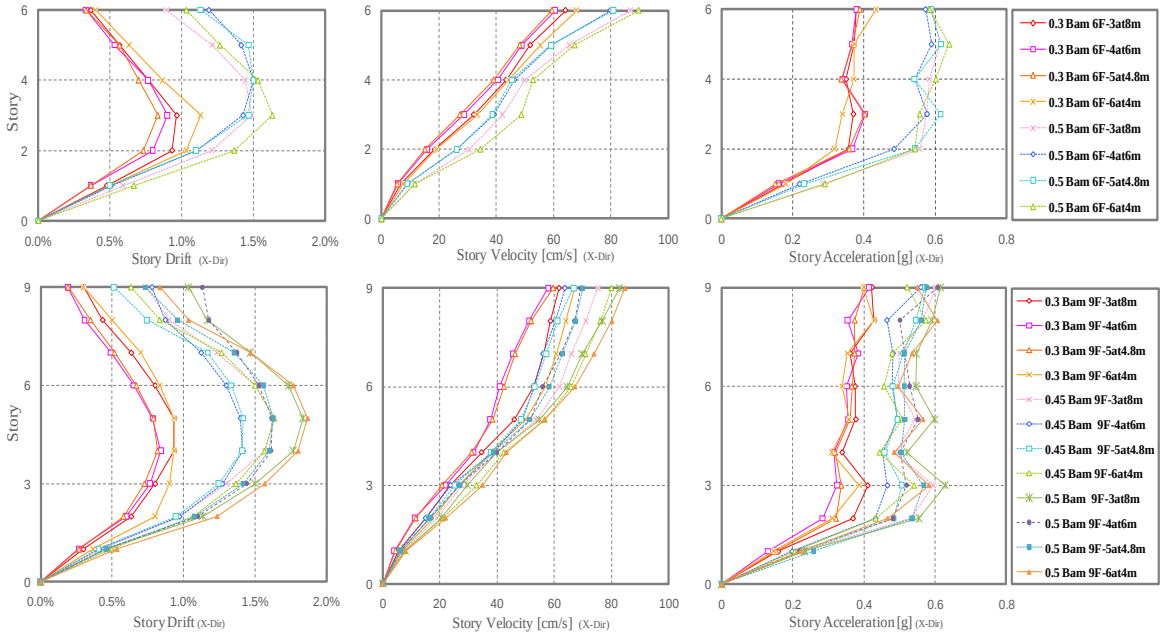

Fig. 17 Maximum story drift, velocity, and acceleration from Bam earthquake

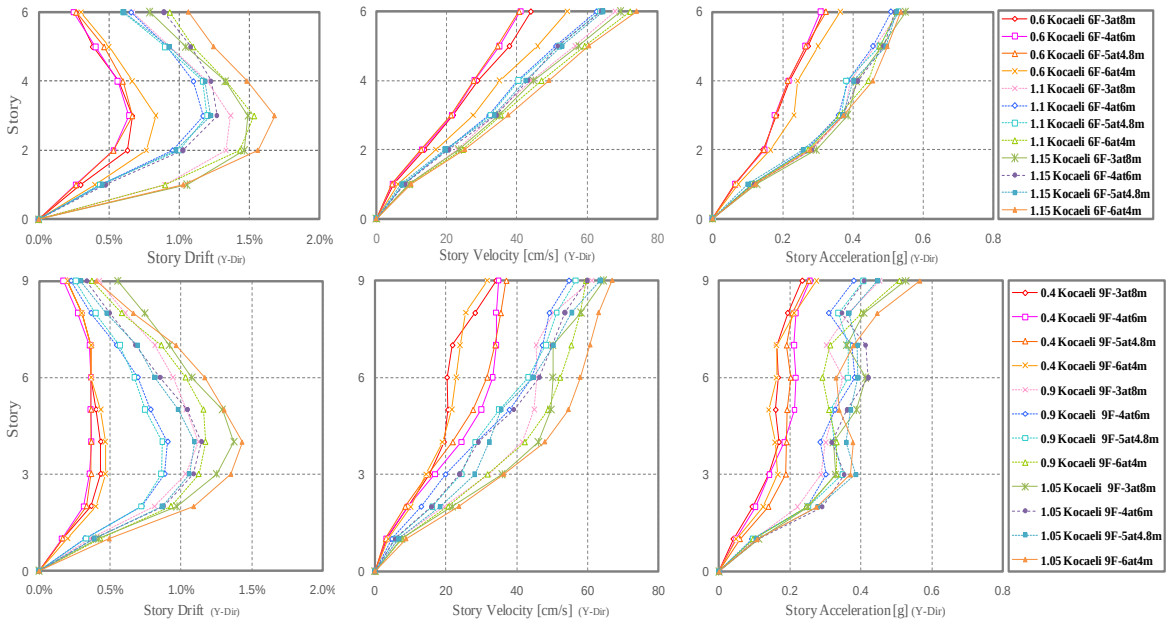

Fig. 17 Maximum story drift, velocity, and acceleration from Bam earthquake

that very strong earthquake records that cause story drift of >2%, do not follow any specific rules. Figs. 16 to 26 reveal that story drift and story velocity for structures with greater R values, which are affected by most of the strong ground motions, are correspondingly lower than for structures

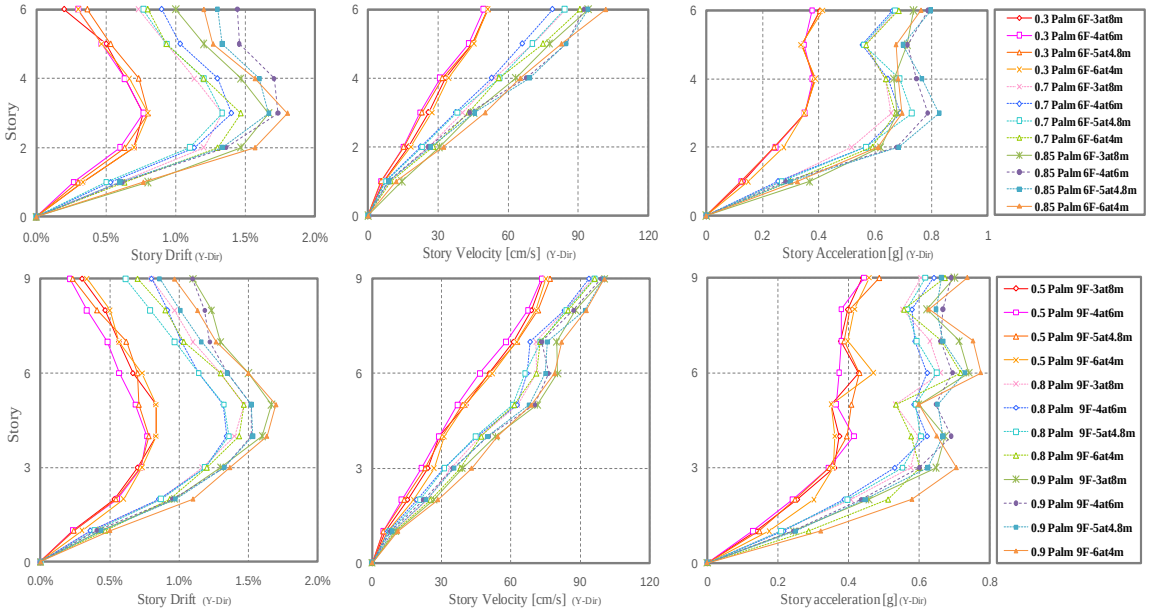

Fig. 18 Maximum story drift, velocity, and acceleration from Kocaeli earthquake

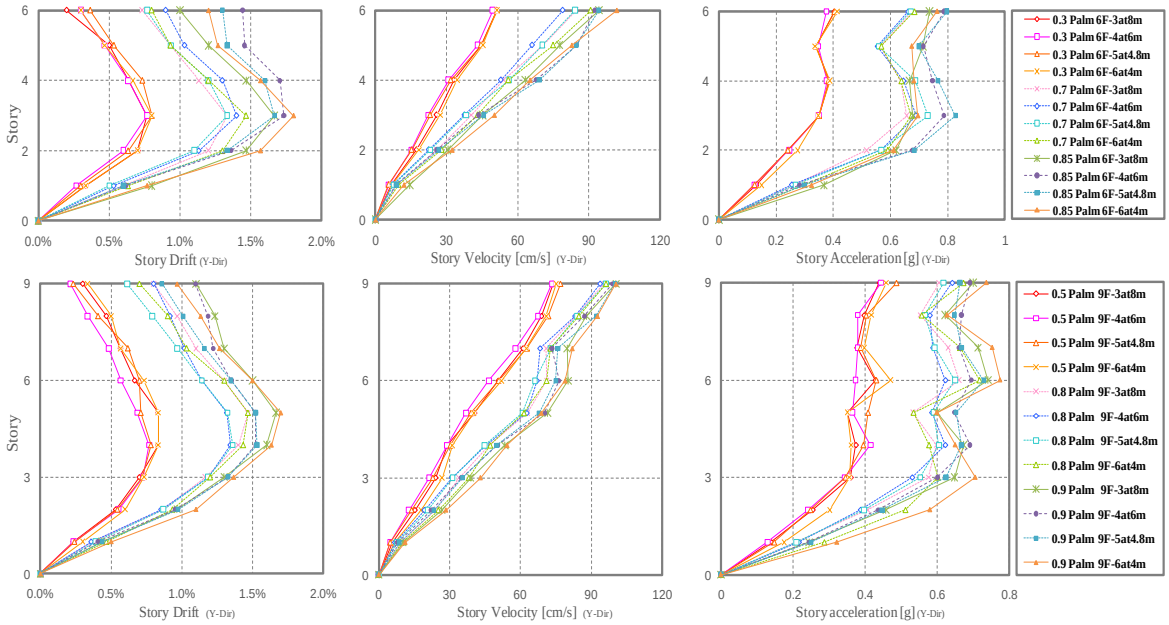

Fig. 19 Maximum story drift, velocity, and acceleration from North Palm Springs earthquake

with smaller *R* values. These results are not applicable to variations in story acceleration.

There are some exceptions related to the results of far field earthquakes. These records are usually weak and require very large scale factors for the records to achieve high performance (after collapse prevention) in incremental dynamic analysis. Applying a large scale factor to far field

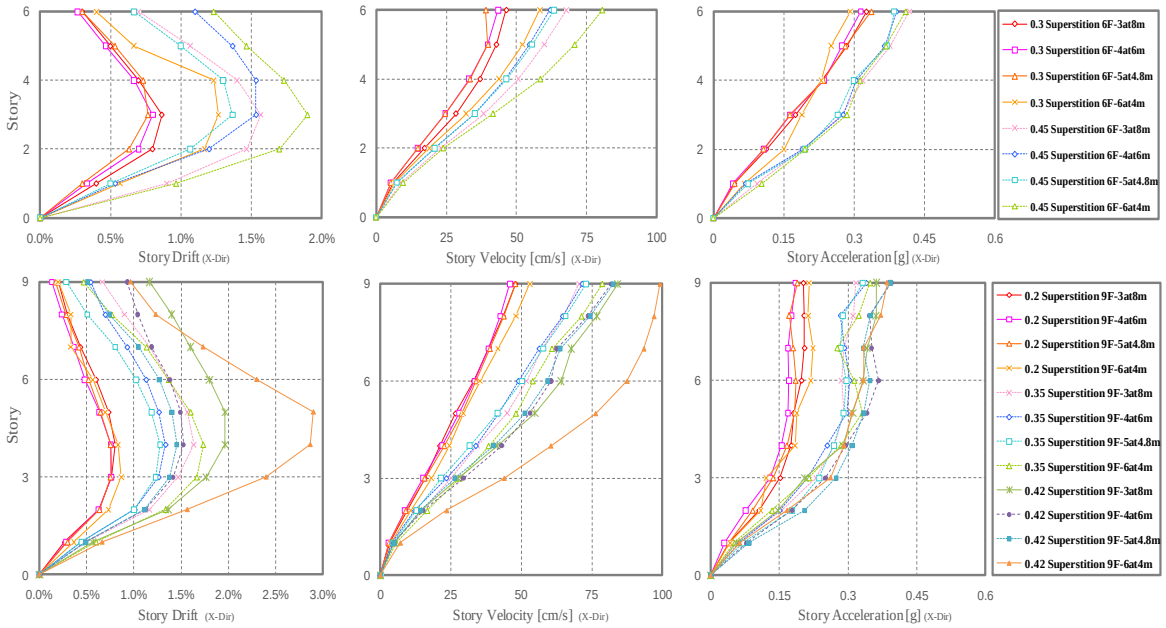

Fig. 20 Maximum story drift, velocity, and acceleration from Superstition Hills earthquake

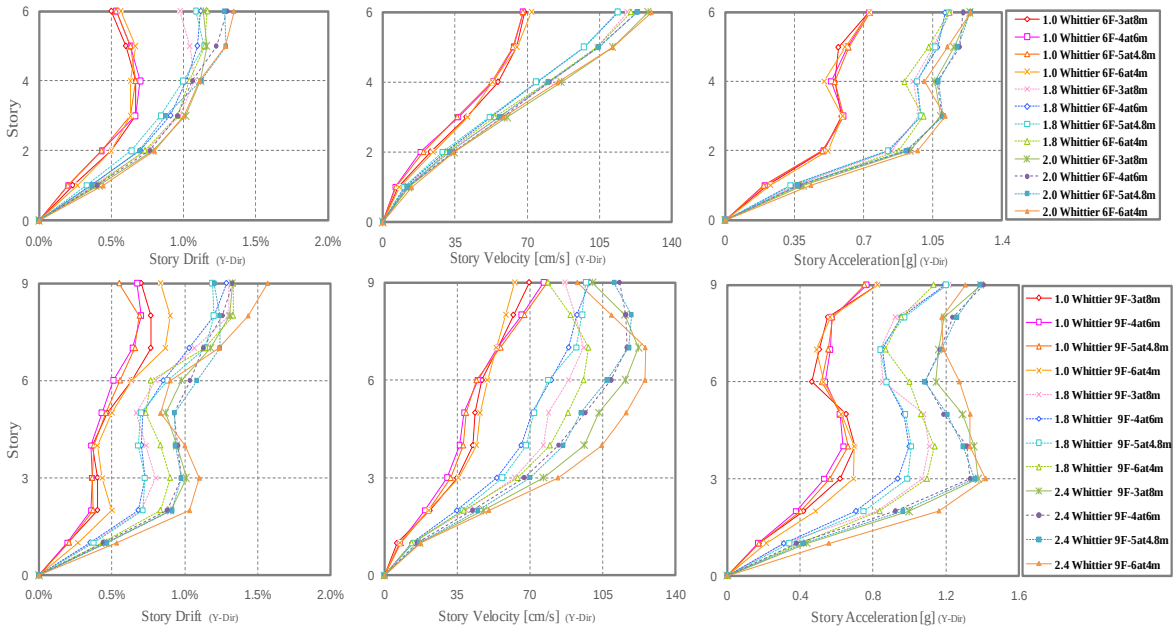

Fig. 21 Maximum story drift, velocity, and acceleration from Whittier Narrows earthquake

records can bolster high-frequency bands in records that cause localized failure and exacerbate the local nonlinearity of structural components.

Changes in story drift for far field earthquakes indicate that the structures will attain the

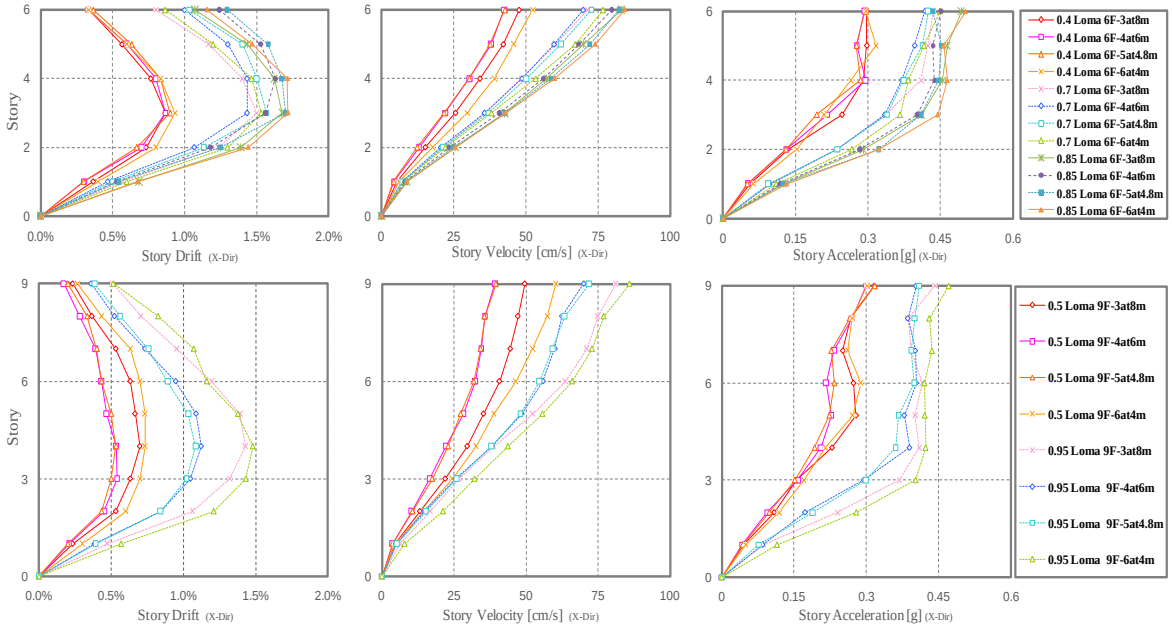

Fig. 22 Maximum story drift, velocity, and acceleration from Loma Prieta earthquake

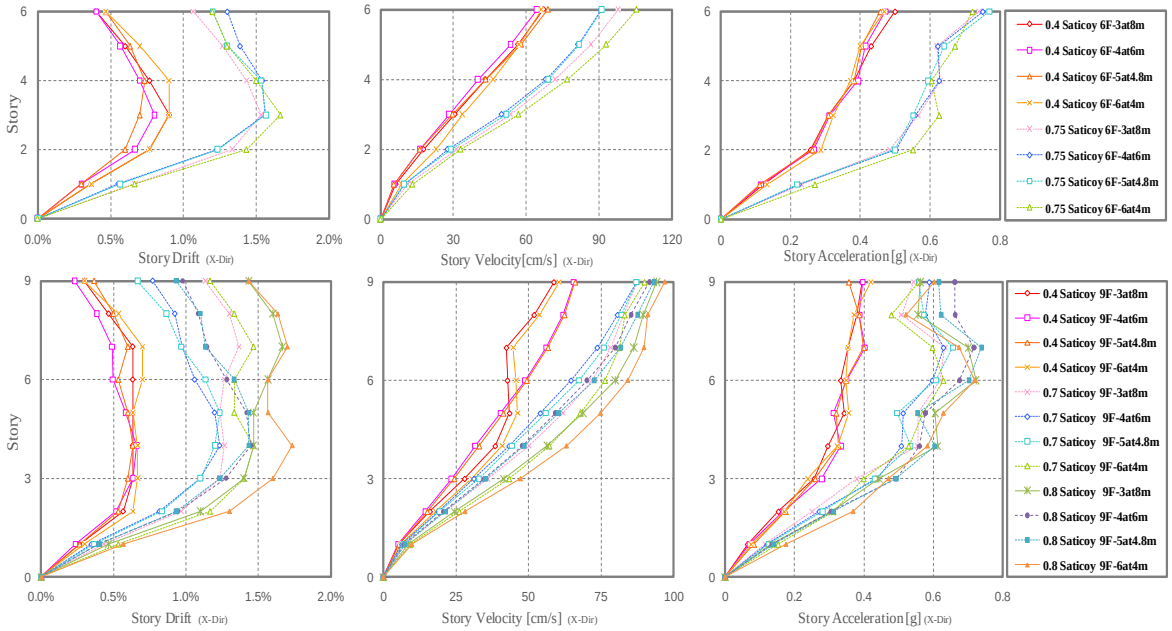

Fig. 23 Maximum story drift, velocity, and acceleration from Northridge Saticoy earthquake

collapse prevention performance level before story drift reaches 1.5%. The existence of strong high-frequency bands in earthquake records indicates that the mechanism of failure in these cases is local failure.

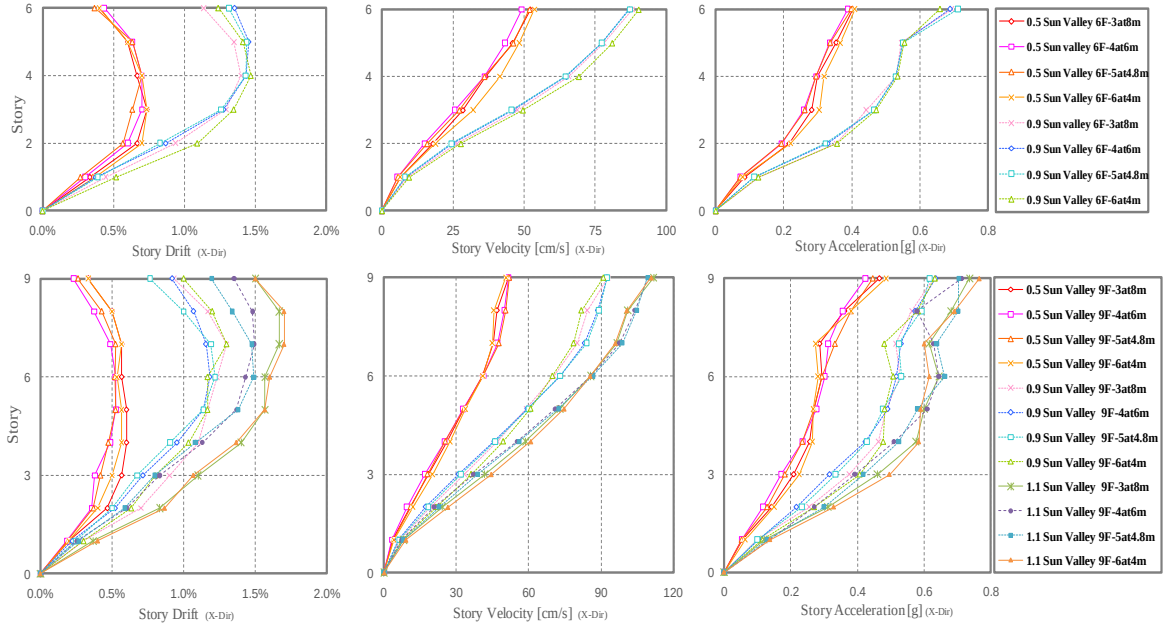

Fig. 24 Maximum story drift, velocity, and acceleration from Northridge Sun Valley earthquake

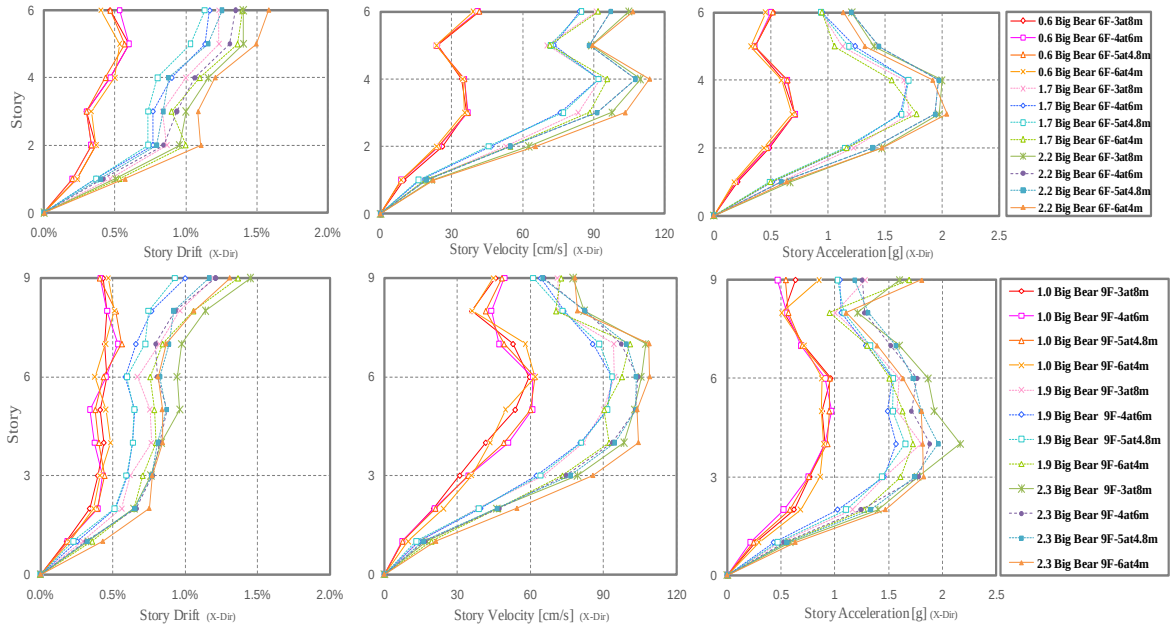

Fig. 25 Maximum story drift, velocity, and acceleration from Big Bear Lake earthquake

8. Conclusions

The present study distinguished between the effects of redundancy and total overstrength in 3D

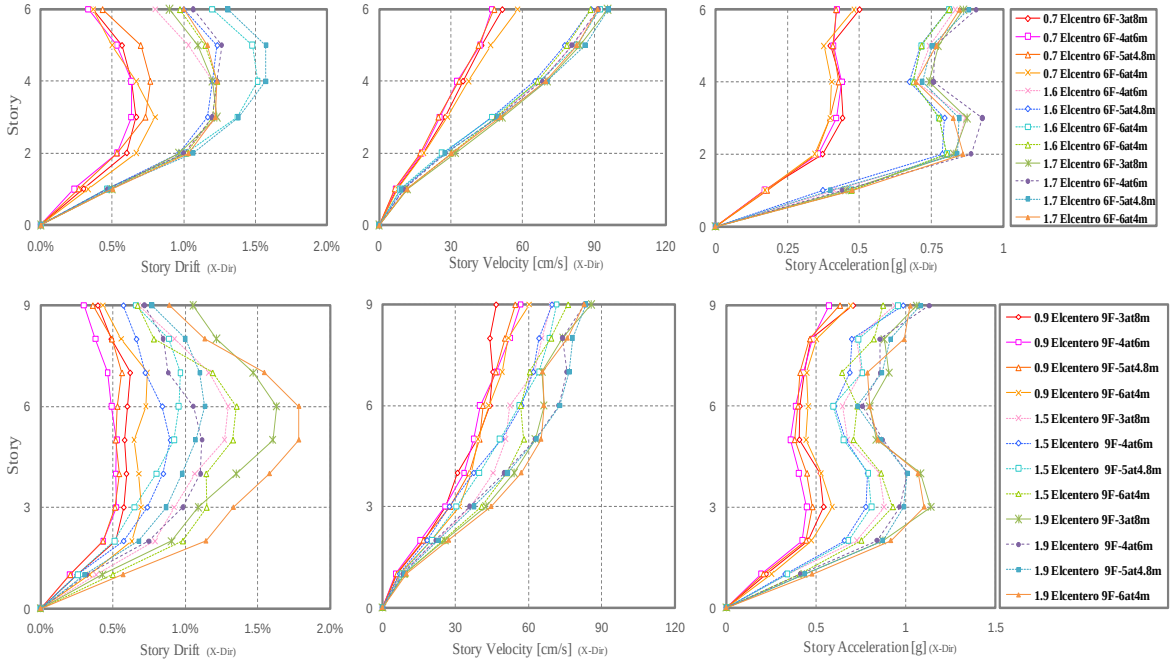

Fig. 26 Maximum story drift, velocity, and acceleration from El Centro earthquake

framed structures which were designed with the ultimate base shear coefficient and equal lateral resistance but different structural redundancy. The effects of redundancy on seismic behavior factor were examined in addition to its effects on the nonlinear behavior of low rise RC framed structures with equal lateral resistance. The results of the numerical analysis of models are:

1. Increasing the number of spans in a fixed plan for moment-resisting frames does not always improve the seismic behavior of structures and increase the seismic behavior factor.
2. The R calculated for lateral monotonic loading can be considered a criterion for the seismic behavior of structures under earthquake loading which creates story drift of ~1.5%. For earthquake loading that results in story drift of >1.5%, structural seismic behavior typically does not follow R.
3. R for the ultimate strength method, when compared with R_w for the allowable strength method, is more consistent with the results of nonlinear dynamic analysis and the response parameters for nonlinear deformation.
4. Story drift and story velocity for the tested models showed that when R decreased, the structural response parameters of the models were smaller than R (within the limits expressed in #2 of the conclusion). This was not observed for story acceleration.
5. The calculated R was not achieved for near field strong ground motion of high amplitude and long period velocity pulses. The conclusion in #4 was not observed for far field strong ground motion with high frequency bands.

References

ATC (1995), *A Critical Review of Current Approaches to Earthquake-Resistant Design,* ATC-34 Report, Applied Technology Council, Redwood City, California.

ATC (1995), *Structural Response Modification Factors, ATC-19 Report*, Applied Technology Council, Redwood City, California.

Bertero, R.D. and Bertero, V.V. (1998), "Redundancy in earthquake-resistant design: how to define it and quantify its effects", *Proceedings of 6th U.S. National Conference on Earthquake Engineering.*

Bertero, R.D. and Bertero, V.V. (1999), "Redundancy in earthquake-resistant design", *J. Struct. Eng.*, **125**, 81-88.

BHRC (2005), *Iranian Code of Practice for Seismic Resistant Design of Buildings*, Standard No. 2800-05. 3rd. Edition, Tehran, Building and Housing Research Center.

Biondini, F., Frangopol, D.M. and Restelli, S. (2008), "On structural robustness, redundancy and static indeterminacy", *Proceedings of the 2008 ASCE-SEI Structures Congress*, Vancouver.

Fallah, A.A., Sarvghad-Moghadam, A. and Massumi, A. (2009), "A nonlinear dynamic based redundancy index for reinforced concrete frames", *J. Appl. Sci.*, **9**(6), 1065-1073.

FEMA (2000), Prestandard and Commentary for Seismic Rehabilitation of Buildings, Federal Emergency Management Agency 356.

Hashemi, S.S., Tasnimi, A.A. and Soltani, M. (2009), "Nonlinear cyclic analysis of reinforced concrete frames, utilizing new joint element", *Scentica iranica*, **16**(6), 490-501.

Husain, M. and Tsopelas, P. (2004), "Measures of structural redundancy in reinforced concrete buildings. I: redundancy indices", *J. Struct. Eng.*, **130**(11), 1651-1658.

Husain, M. and Tsopelas, P. (2004), "Measures of structural redundancy in reinforced concrete buildings. ii: redundancy response modification factor R_R", *J. Struct. Eng.*, **130**(11), 1659-1666.

IBC 2000 (1998), *International Building Codes*, Inter, Code Council, Falls Church, VA.

Iranian National Building Code (2010), *Design Loads for Buildings*, Part 6, INBC, National Building Regulations Office, Tehran, Iran.

Kalkan, E. and Kunnath, S.K. (2007), "Effective cyclic energy as a measure of seismic demand", *J. Earthq. Eng.*, **11**, 725-751.

Liao, K.W. and Wen, Y.K. (2004), "Redundancy in steel moment frame systems under seismic excitation", Department of Civil and Environmental Engineering, University of Illinois at Urbana-Champaign Illinois, August.

Marhadi, K. and Venkataraman, S. (2009), "Surrogate measures to optimize structures for robust and predictable progressive failure", *Struct. Multidisc. Optim.*, **39**, 245-261.

Massumi, A. and Tasnimi, A.A. (2006), "Estimation of response modification factors for RC moment resisting frames", Building and Housing Research Center, Publication R-436, Tehran, Iran.

Mirenda, E. and Bertero, V.V. (1994), "Evaluation of Strength Reduction Factors For Earthquake-Resistant Design", *Earthq. Spectra*., **10**(2), 357-379.

Mohammadi, R., Massumi, A. and Meshkat-Dini, A. (2015), "Structural reliability index versus behavior factor in RC frames with equal lateral resistance", *Eartheq. Struct.*, **8**(5), 996-1016.

Okasha, N.M. and Frangopol, D.M. (2010), "Time-variant redundancy of structural systems", *J. Struct. Infrastr. Eng.*, **6,** 279-301.

Park, R. (1989), "Evaluation of ductility of structures and structural assemblages from laboratory testing", *Bull. NZ. Nat. Soc. Earthq. Eng.*, **22**(3), 155-166.

SAP2000 (2010), Version 14.2.0, A Computer Program for Integrated Finite Element Analysis and Design of Structures, University of California, Berkeley.

Song, S.H. and Wen, Y.K. (2000), "Structural redundancy of dual and steel moment frame systems under seismic excitation", A Report on a Research Project sponsored by the National Science Foundation (Grant NSF EEC-97-01785), University of Illinois at Urbana- Illinois, November.

Uang, C.M. (1991), "Establishing R and Cd factors for building seismic provisions", *J. Struct. Eng.*, **117**(1),

19-28.
Wen, Y.K. and Song, S.H. (2003), "Structural reliability/redundancy under earthquakes", *J. Struct. Eng.*, **12**(1), 56-66.
Yoshihiro, K. and Yakov, B.H. (2011), "Redundancy and robustness, or when is redundancy redundant?", *J. Struct. Eng.*, **137**(9), 935-945..

CC